

# MOOSE Project: Part 3

Mohamed AbdulHameed

April 2023

## 1 Computational details

Two MOOSE input files have been prepared to calculate the stress in a cylindrical  $\text{UO}_2$  fuel rod due to the thermal expansion of the fuel:

1. Using temperature-dependent thermal conductivity according to the correlation:

$$k = \frac{1}{3.8 + 0.0217 T} \quad (1)$$

due to the way MOOSE handles the temperature-dependent thermal conductivity, Eq. 1 has been fitted to a line of the form:

$$k = k_0 (1 + \alpha T) \quad (2)$$

in the temperature range 650-1500 K, with  $k_0 = 0.07298$  W/cm-K and  $\alpha = -0.000438$  1/K.

2. Using a constant thermal conductivity of 0.038 W/cm-K which has been calculated from:

$$k_{\text{av}} = \frac{1}{1500 - 650} \int_{650}^{1500} \frac{1}{3.8 + 0.0217 T} dT \quad (3)$$

For  $\text{UO}_2$ , a specific heat of 0.33 J/g-K, a density of 10.98 g/cm<sup>3</sup>, a Young's modulus of 250 GPa, a Poisson's ratio of 0.32, a linear thermal expansion coefficient of  $10.471 \times 10^{-6}$  1/K [1, 2] were used in both input parameters.

Both the radial (0.5 cm) and the axial direction (100 cm) has 20 mesh points. 10 and 30 mesh points were used in both directions without a significant change in the results. A time-independent, axially variant linear heating rate (LHR) was used in both calculations, which has the form:

$$\text{LHR} = 350 \cos \left( 1.208 \left( \frac{z}{50} - 1 \right) \right) \quad (4)$$

In this calculation, both the Heat Conduction and Tensor Mechanics modules were coupled. Normally, the heat flow moves much more slowly than the solid mechanics response. Therefore, the input must have a time derivative in the heat conduction equation but none for the solid mechanics so that at each time step the solid mechanics is solved to a full steady state based on the current configuration of heat. Such a configuration is called quasi-transient, solved in MOOSE via the transient executioner. That is, a steady-state simulation is not possible for a coupled thermo-mechanics problem.

The fuel surface temperature was set to 650 K and treated as a boundary condition. For the axial displacement, it was set to zero at the bottom of the fuel rod, whereas the radial displacement was set to zero only at the origin; a procedure known as pinning. Pinning at a single point is less restrictive and allows the model to freely expand, while still removing all rigid body motion, i.e., translation and rotation. Removing translation requires fixing the  $r$  and  $z$  displacements on at least one node, whereas removing rotations requires fixing  $r$  or  $z$  displacements (not necessarily both) on another node.

For the transient solution, the Single Matrix Preconditioner (SMP) and the Precondition Jacobian-Free Newton Krylov (PJFNK) solver were used. The transient problem was run for 50 s with an adaptive time stepper whose initial time step was set to 1 s. The time step kept increasing up to about 4 s at the end of the simulation. It is worth noting that the MOOSE adaptive time stepper only decreases in cases of non-convergence.

## 2 Results

The results are shown in Fig. 1-7. A few comments about the results are in order:

- The temperature rise along the fuel rod is larger in the constant  $k$  model than it is in the  $T$ -dependent  $k$  model. That is, the constant  $k$  model overestimates the temperature rise and can be considered a conservative initial estimate in fuel design.
- The radial stress is totally compressive in both cases as expected.
- The hoop and axial stresses are compressive near the centerline and undergo a turnover to become tensile near the fuel rod surface.
- For the fuel rod the stress is higher at  $z = 50$  cm when the temperature is higher due to the LHR profile, and decreases as we move away from the center.
- Despite the large difference between the temperature profile for the constant  $k$  and  $T$ -dependent  $k$  cases, the stress in the first case is only slightly larger in magnitude than the second case.

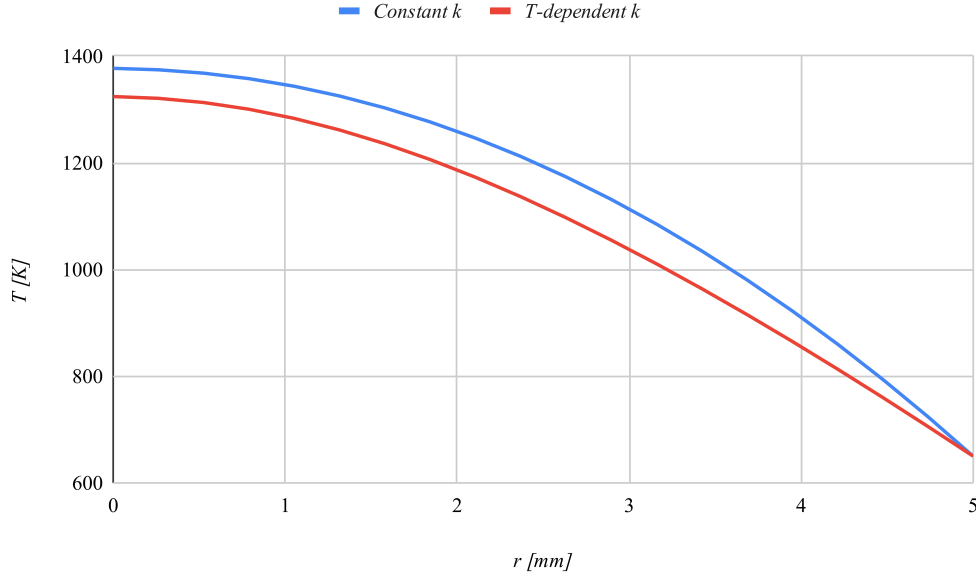


Figure 1: The variation of  $T$  with  $r$  at  $z = 50$  cm for both constant  $k$  and  $T$ -dependent  $k$ .

## References

1. Terrani, K. A., Balooch, M., Burns, J. R. & Smith, Q. B. Young's modulus evaluation of high burnup structure in  $\text{UO}_2$  with nanometer resolution. *Journal of Nuclear Materials* **508**, 33–39. ISSN: 0022-3115 (Sept. 2018).
2. Kang, K. H., Ryu, H. J., Song, K. C. & Yang, M. S. Thermal expansion of  $\text{UO}_2$  and simulated DUPIC fuel. *Journal of Nuclear Materials* **301**. ISSN: 00223115 (2-3 2002).

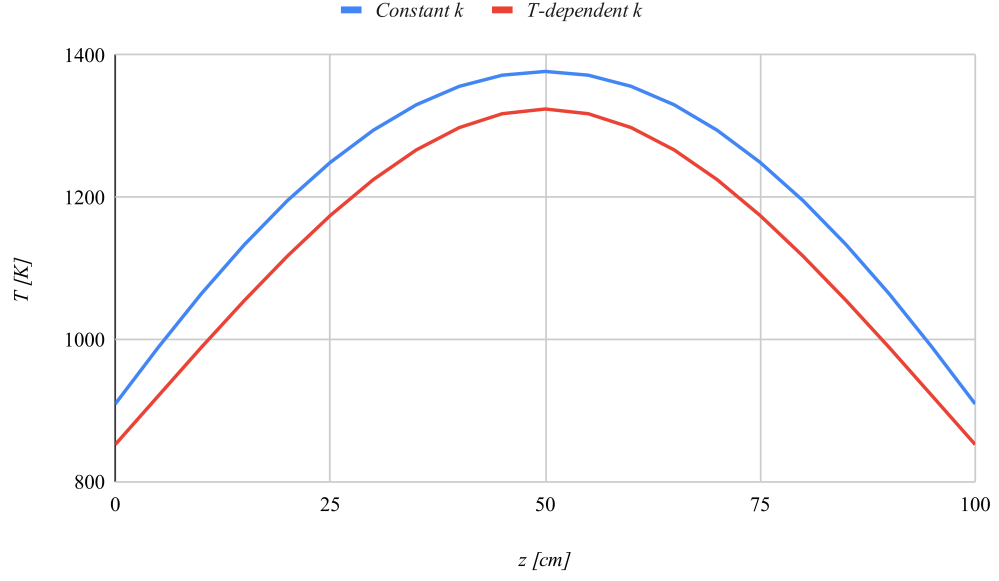


Figure 2: Centerline  $T$  for both constant  $k$  and  $T$ -dependent  $k$ .

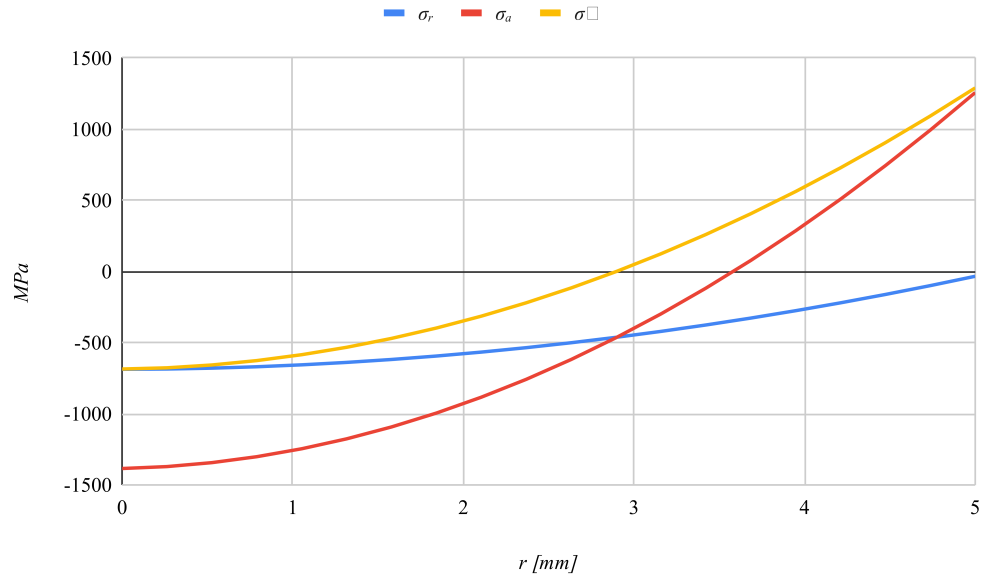


Figure 3: Radial  $\sigma_r$ , axial  $\sigma_a$ , and hoop  $\sigma_\theta$  stresses at  $z = 50$  cm for constant  $k$ .

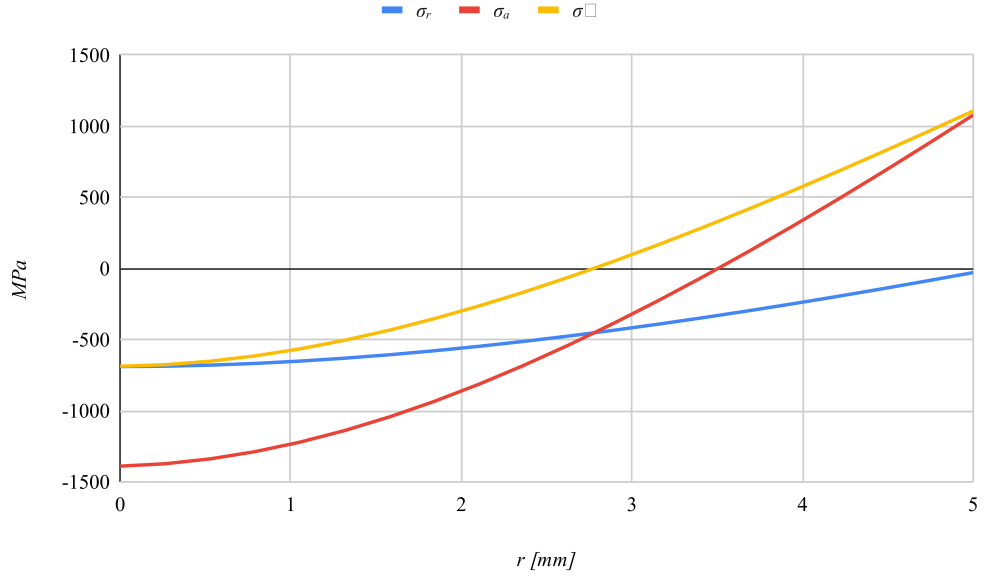


Figure 4: Radial  $\sigma_r$ , axial  $\sigma_a$ , and hoop  $\sigma_\phi$  stresses at  $z = 50$  cm for  $T$ -dependent  $k$ .

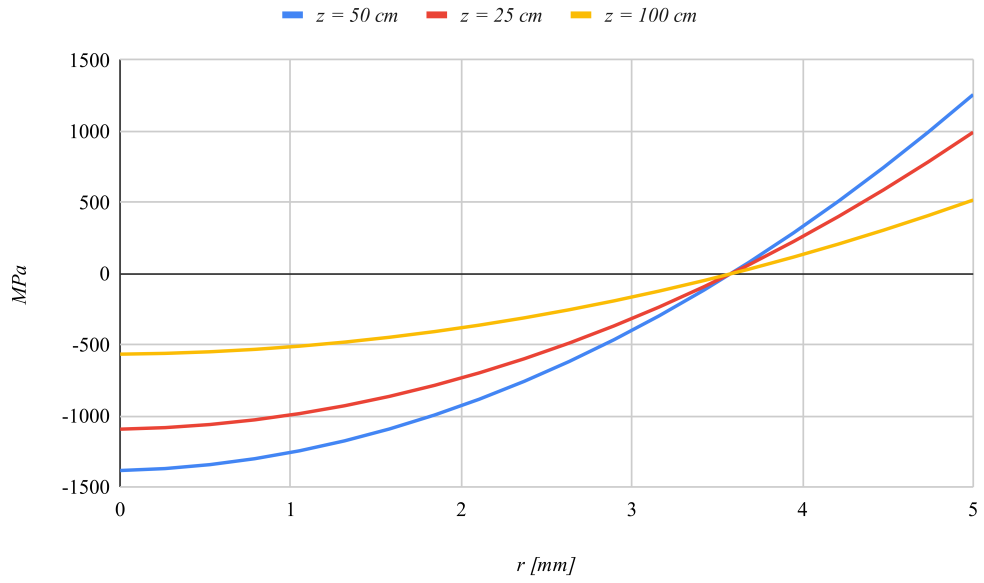


Figure 5: Axial stress at different  $z$  for constant  $k$ .

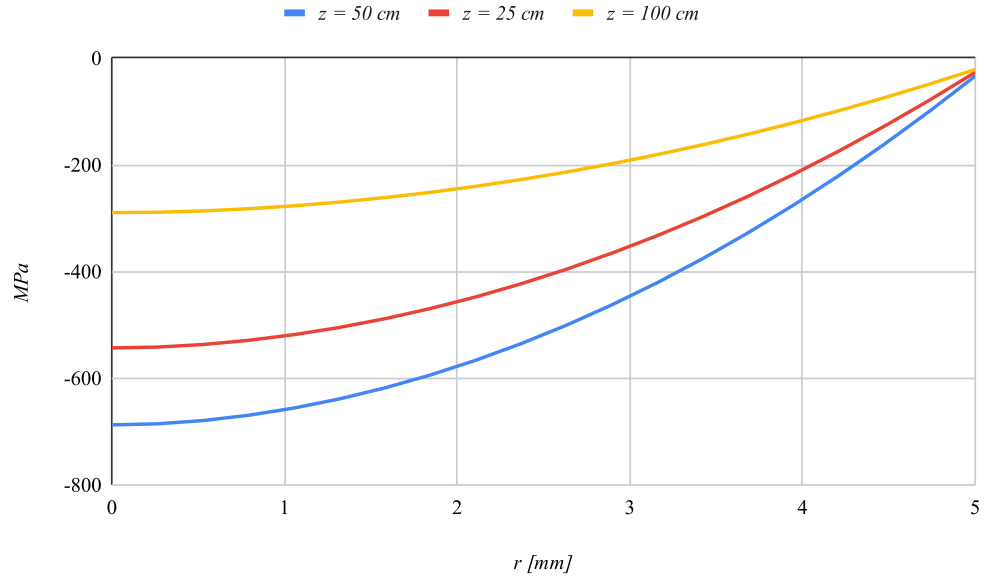


Figure 6: Radial stress at different  $z$  for constant  $k$ .

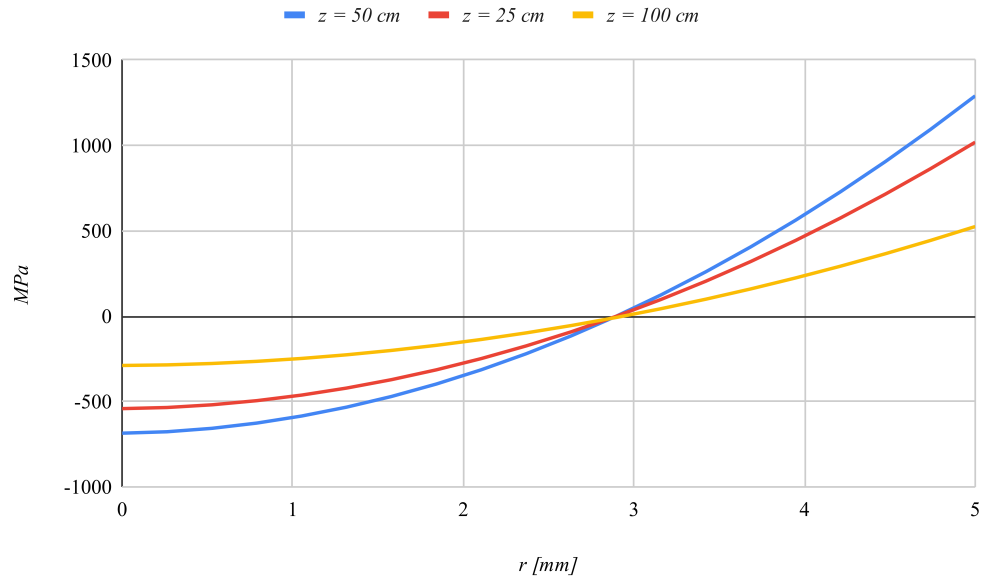


Figure 7: Hoop stress at different  $z$  for constant  $k$ .

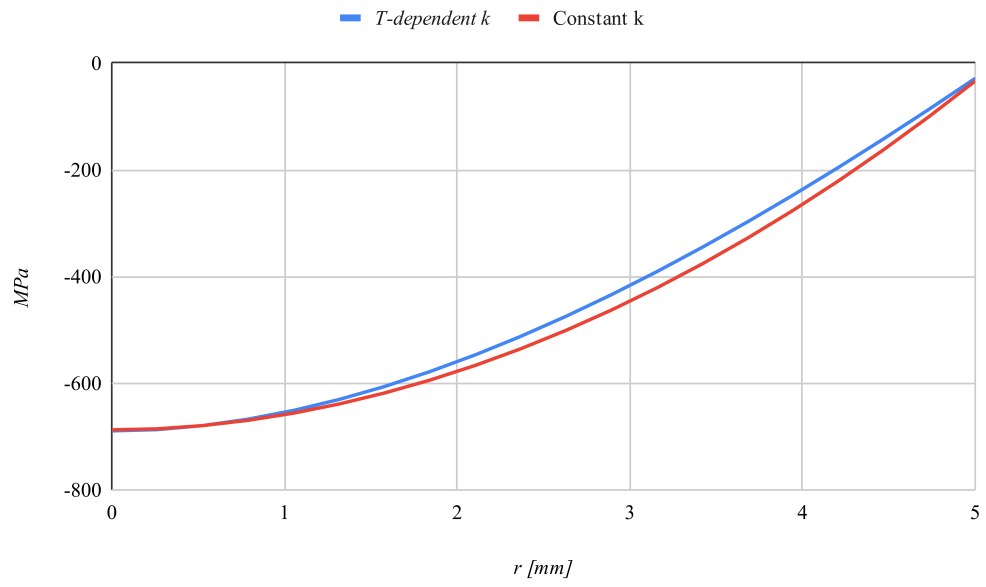


Figure 8: Radial stress at  $z = 50$  cm for both constant  $k$  and  $T$ -dependent  $k$ .